



University of Wisconsin - Madison

MAD/PH/859
hep-ph/9504425

Comparison of potential models through HQET

James F. Amundson*

*Department of Physics, University of Wisconsin,
Madison WI 53706*

Abstract

I calculate heavy-light decay constants in a nonrelativistic potential model. The resulting estimate of heavy quark symmetry breaking conflicts with similar estimates from lattice QCD. I show that a semirelativistic potential model eliminates the conflict. Using the results of heavy quark effective theory allows me to identify and compensate for shortcomings in the model calculations in addition to isolating the source of the differences in the two models. The results lead to a rule as to where the nonrelativistic quark model gives misleading predictions.

*e-mail: amundson@phenom.physics.wisc.edu

1 Introduction

The nonrelativistic quark model is one of the oldest and most successful models of hadronic physics. This success is somewhat puzzling in that it persists even when the model is applied to light quark hadrons, where the dynamics are dominantly relativistic. Perhaps more puzzling is that relativistic corrections to the nonrelativistic quark model do not to substantially improve the model's predictions for spectra [1]. Some (but not all) of the ideas of the nonrelativistic quark model for heavy-light systems gain a stronger theoretical basis through heavy quark effective theory (HQET). In this work I show how the nonrelativistic quark model can be used in conjunction with HQET to calculate heavy-light decay constants. By doing the same calculation with a semirelativistic potential model, I show how relativistic extensions of the simple quark model can make a dramatic improvement in some types of calculations. This, in turn, indicates which nonrelativistic quark model calculations should not be trusted.

Before turning to the model calculations it is important to understand what HQET tells us about decay constants, since HQET provides the only results that follow directly from QCD. The application of the ideas of HQET to heavy-light decay constants preceded the development of the effective theory itself. The nonrelativistic quark model led to the prediction that heavy-light decay constants follow the scaling behavior [2]

$$f_M \propto \frac{1}{\sqrt{m_M}}. \quad (1)$$

Later, Shifman and Voloshin [3] and, separately, Politzer and Wise [4] calculated the leading-logarithmic corrections to Eq. (1)

$$\frac{f_B}{f_D} = \left[\frac{\alpha_s(m_c)}{\alpha_s(m_b)} \right]^{6/25} \sqrt{\frac{m_D}{m_B}} \quad (2)$$

in a model-independent manner, *i.e.*, following directly from QCD in the limit where the heavy quark mass goes to infinity while the the QCD scale remains fixed.

The above relation is of both theoretical and practical interest. Theoretically, Eq. (2) is interesting because it is a model-independent prediction of QCD in a well-defined limit. Practically, it is interesting because f_B is an input to other calculations, such as B^0 - \bar{B}^0 mixing. Unfortunately, a direct measurement of f_B through leptonic decay will be extremely challenging because of the very small branching ratio and difficult signature. A measurement of f_D , on the other hand, is much more feasible. In fact, measurements of f_{D_s} , which is related to f_D by flavor SU(3), are already available [5, 6, 7], albeit with large errors.

Unfortunately, in the real world the bottom and, particularly, the charm quark masses are quite finite compared to the QCD scale. It is therefore necessary to consider the finite-mass corrections to Eq. (2). The predictive power of the effective theory vanishes when the leading-order finite mass corrections the decay constants are included. This means the size of the corrections must be estimated using lattice QCD or some model. This problem has been studied extensively on the lattice [8, 9, 10, 11], where results indicate that the corrections to the heavy quark limit for f_B are $\mathcal{O}(\epsilon\%)$, which corresponds to a subleading heavy quark term of size $(1 \text{ GeV})/m_Q$. QCD sum rules [12] are consistent with these lattice results. The large correction is surprising when compared to what one would naively expect from the nonrelativistic quark model, something like $(0.3 \text{ GeV})/m_Q$. Naive estimates can miss factors of three, of course. It is necessary to do an explicit calculation to see that the nonrelativistic quark model really conflicts with the lattice calculations.

This work uses two simple potential models to explicitly calculate decay constants in the heavy quark limit and beyond. The first, hereafter referred to as the “nonrelativistic quark model” is based on the Hamiltonian of the Isgur-Scora-Grinstein-Wise (ISGW) model [13] in the heavy quark limit. This model is very simple, in contrast to lattice methods, which are rigorous, but also exceedingly complicated. Even if the lattice is able to provide precise answers to the structure of hadrons, it is useful to find simple pictures which describe the important physics. The second model, the “semirelativistic quark model” is an simple generalization of the first. The difference is substitution of the relativistic form for the kinetic energy for the

nonrelativistic form used in the ISGW model. This simple change involves subtleties which are discussed in the body of the text.

One might reasonably ask, given a willingness to use these models for calculations, why bother with HQET at all? There are several reasons. The first is that HQET provides some checks on the calculation. At subleading order, HQET does show that there is a term missing from the model calculation. Fortunately, it is a term that may be added by hand. A second reason is that HQET allows the inclusion of radiative corrections in a rigorous manner. Finally, and perhaps most importantly, HQET provides a *detailed* way to compare models. When models differ in their predictions, it is desirable to isolate the regions in which they differ. Unfortunately, when one takes apart two different models to compare, it becomes a matter of comparing apples and oranges. By calculating nonperturbative matrix elements that arise in HQET, the two models can be compared in a physically meaningful way.

The next section reviews the HQET predictions for decay constants to subleading order in $1/m_Q$. The following sections describe the calculations in the nonrelativistic and semirelativistic models. I then compare the results of the two models and discuss the implications for other nonrelativistic quark model calculations. The appendix describes the numerical methods I used to do the calculations.

2 HQET for meson decay constants

The heavy quark effective Lagrangian [14, 15],

$$\mathcal{L}_{\text{HQ}} = \bar{h}_v D \cdot v h_v, \quad (3)$$

is by now well known. For a review which includes an extensive discussion of decay constants, see Ref. [16]. The spin and heavy quark mass symmetries of the heavy quark limit are manifested by the lack of gamma matrices and masses in Eq. (3). The usual definition of the pseudoscalar decay constant, f_M , of a $Q\bar{q}$ meson M with four-momentum p is

$$\langle 0 | A_\mu | M(p) \rangle = i f_M p_\mu, \quad (4)$$

where A_μ is the axial current. Throughout this work M (M^*) represents a heavy-light pseudoscalar (vector) meson with a heavy quark Q and a light antiquark \bar{q} . Using the symmetries of Eq. (3), one can see that in the heavy quark limit

$$f_M \sqrt{m_M} = F, \quad (5)$$

where F is a universal dimensionful parameter of QCD. This parameter depends on the nonperturbative sector of QCD, so it is not currently calculable from first principles. (It is calculable on the lattice in principle.) In the symmetry limit, *i.e.*, when the bottom and charm quarks are taken to be infinitely massive, the decay constants of the D , D^* , B and B^* are determined by F .

The discussion so far ignores radiative corrections. When the leading-logarithmic radiative corrections to the axial current in the heavy quark limit are included, the result becomes

$$f_M \sqrt{m_M} = \left[\frac{\alpha_s(\mu)}{\alpha_s(m_Q)} \right]^{\frac{2}{\beta_0}} F(\mu), \quad (6)$$

where $\beta_0 = (33 - 2n_f)/3$. The general form of the result is $C(\mu)F(\mu)$, where $C(\mu)$ is the perturbative coefficient to the low-energy parameter $F(\mu)$. Since physics does not depend on the choice of scale, the μ -dependence of the product must vanish.

At subleading order in $1/m_Q$ and including leading-log radiative corrections, the Lagrangian grows [17, 18, 19]:

$$\mathcal{L}_{\text{QCD}} = \mathcal{L}_{\text{HQ}} + \frac{1}{2m_Q} \bar{h}_v D^2 h_v + \frac{1}{4m_Q} \left[\frac{\alpha_s(\mu)}{\alpha_s(m_Q)} \right]^{-\frac{3}{\beta_0}} \bar{h}_v g_s \sigma^{\mu\nu} G_{\mu\nu} h_v + \mathcal{O} \left(\frac{\Lambda_{\text{QCD}}^2}{m_Q^2} \right). \quad (7)$$

A third term at order $1/m_Q$ whose matrix elements vanish due to the equations of motion has been omitted. The first correction term is the leading part of the kinetic energy of the heavy quark. Its perturbative coefficient is unity because of reparameterization invariance [20]. The second correction term arises from the heavy quark's non-zero chromomagnetic moment. These terms give rise to corrections to the decay constant through modifications of the meson wave function and of the heavy-light current. When these effects are included, the simple result in Eq. (5) becomes (ignoring radiative corrections for simplicity) [21]

$$f_M \sqrt{m_M} = F \left\{ 1 + \frac{1}{m_Q} [G_1 + 2d_M G_2] - d_M \frac{\tilde{\Lambda}}{6m_Q} \right\}, \quad (8)$$

where $d_M = +3$ (-1) for pseudoscalar (vector) mesons. Here the effect of the modification to the meson wave function due to the kinetic energy term and the chromomagnetic term are parameterized by G_1 and G_2 , respectively. The finite difference between the heavy *quark* momentum and the heavy *meson* momentum gives rise to the final term. G_1 , G_2 and $\tilde{\Lambda}$ are dimensionful parameters of QCD which, like F , cannot be calculated in perturbation theory.

Unlike G_1 and G_2 , the parameter $\tilde{\Lambda}$ is directly related to other heavy quark processes. The difference between the mass m_M of a heavy-light meson and the corresponding heavy quark mass m_Q is conventionally defined as

$$\bar{\Lambda} = m_M - m_Q. \quad (9)$$

$\tilde{\Lambda}$ is related to $\bar{\Lambda}$ by [16]

$$\tilde{\Lambda} = \bar{\Lambda} - m_q, \quad (10)$$

where m_q is the *light* quark mass. Since the current masses of the up and down quarks (5–10 MeV) are considerably smaller than estimates of $\bar{\Lambda}$ (typically 300–700 MeV), $\tilde{\Lambda}$ is usually taken to be equal to $\bar{\Lambda}$. A subtlety which arises in the model calculations in the following sections makes this distinction important.

Including the leading-log radiative corrections to Eq. (8),

$$f_M \sqrt{m_M} = \left[\frac{\alpha_s(\mu)}{\alpha_s(m_Q)} \right]^{\frac{2}{\beta_0}} F(\mu) \left\{ 1 + \frac{1}{m_Q} \left[G_1(\mu) + 2d_M \left[\frac{\alpha_s(\mu)}{\alpha_s(m_Q)} \right]^{\frac{3}{\beta_0}} G_2(\mu) \right] - \frac{\tilde{\Lambda}}{6m_Q} \left[\frac{16}{\beta_0} \ln \frac{\alpha_s(\mu)}{\alpha_s(m_Q)} + d_M \frac{16}{9} \left[\frac{\alpha_s(\mu)}{\alpha_s(m_Q)} \right]^{\frac{3}{\beta_0}} \right] \right\}. \quad (11)$$

An important point about the above complicated expression is that the $G_1(\mu)$ term has the same perturbative coefficient as $F(\mu)$ because of reparameterization invariance, while the $G_2(\mu)$ term gets a non-trivial perturbative coefficient.

At this level the results of HQET have lost their beautiful simplicity. Unfortunately, they have also lost their predictive power because the four decay constants $f_{D^{(*)}}$, $f_{B^{(*)}}$ are given in terms of four unknown parameters F , G_1 , G_2 and $\tilde{\Lambda}$. Of these, only $\tilde{\Lambda}$ is obtainable from other heavy-meson processes in principle. The task for the model calculations is to estimate these parameters.

3 Nonrelativistic Model Calculation

In the nonrelativistic quark model, meson decay constants are given by [22, 23, 24, 25, 26]

$$f_M \sqrt{m_M} = \sqrt{12} |\psi_M(\mathbf{r} = 0)|. \quad (12)$$

The “non-relativistic quark model” for this paper is a heavy constituent quark Q bound to a light antiquark \bar{q} obeying the Hamiltonian

$$\mathcal{H} = \frac{p^2}{2m_q} + \frac{p^2}{2m_Q} - \frac{4\alpha_s}{3r} + ar + \frac{8\pi\alpha_s \mathbf{S}_Q \cdot \mathbf{S}_q}{3m_q m_Q} \delta^3(\mathbf{r}). \quad (13)$$

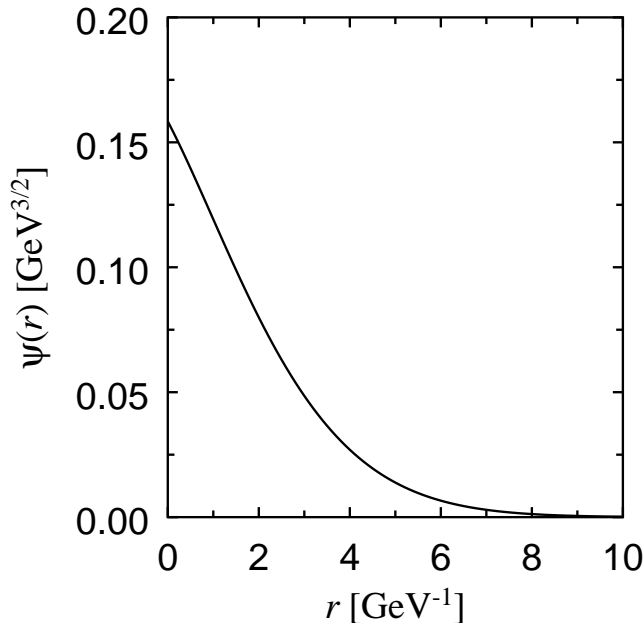


Figure 1: Nonrelativistic wave function.

The last three terms in the Hamiltonian are the quark-antiquark potential. The first and third represent the coulomb-like and hyperfine effects of single gluon exchange, respectively. The linear term is a phenomenological spin-independent confining potential. A more general Hamiltonian would also include spin-orbit coupling terms. I have omitted such terms because all of the calculations in this work involve only S -wave states for which spin-orbit contributions vanish. Without the hyperfine term, the Hamiltonian is that of the ISGW model [13]. With the hyperfine term, the model is closely related to the updated model of Isgur and Scora (ISGW2) [27]. It should be noted that this model differs from ISGW and ISGW2 in that I use exact (numerical) wave functions, while the others use simple variational wave functions. While variational wave functions are useful for the calculations in ISGW and ISGW2, which involve overlaps of wave functions, they are not appropriate for decay constants, which are sensitive to the wave function at a single point.

As the heavy quark mass is taken to infinity, expectation values of p and $\delta^3(\mathbf{r})$ remain of order of the QCD scale. In this limit the above Hamiltonian reduces to [28]

$$\mathcal{H}_\infty = \frac{p^2}{2m_q} - \frac{4\alpha_s}{3r} + ar. \quad (14)$$

Solving the Schrödinger equation

$$\mathcal{H}_\infty \phi_\infty^{\text{NR}} = E \phi_\infty^{\text{NR}} \quad (15)$$

for the ground state wave function and comparing with Eq. (12) gives

$$F = \sqrt{12} |\phi_\infty^{\text{NR}}(\mathbf{r} = 0)|. \quad (16)$$

This model calculation explicitly obeys the mass and spin symmetries of the heavy quark effective theory. Solving Eq. (15) numerically gives $F = 0.55 \text{ GeV}^{3/2}$. I have used the parameter values $m_q = 330 \text{ MeV}$, $\alpha_s = 0.5$, $a = 0.18 \text{ GeV}^2$ from Ref. [13]. Figure 1 displays the calculated wave function. Unfortunately, numerical calculations such as this tend to obscure the dependence of the results on the input parameters. This is particularly important when trying to establish agreement or disagreement between different types of calculations. Figure 2 makes the parameter dependence of the result more explicit by displaying the dependence of F on the input parameters within $\pm 50\%$ of each nominal value.

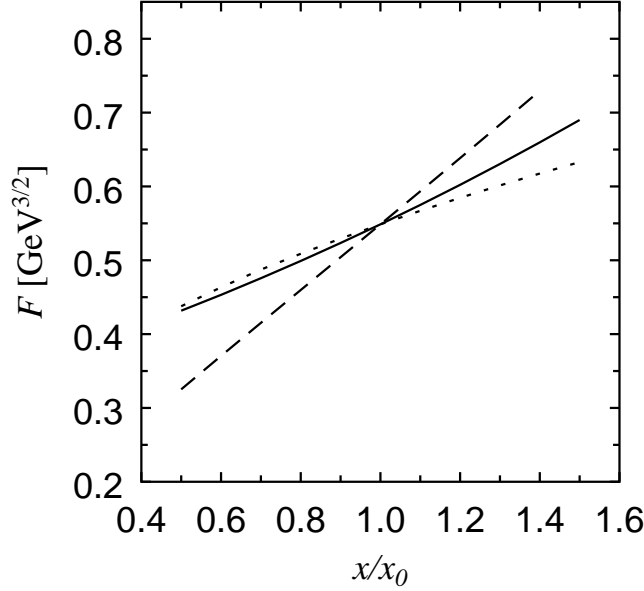


Figure 2: Parameter dependence of F calculated using the nonrelativistic model. The nominal values (x_0) are (solid line) $\alpha_s = 0.5$, (dashed line) $m_q = 0.33$ GeV, and (dotted line) $a = 0.18$ GeV².

In order to calculate the decay constant to subleading order in $1/m_Q$, it is necessary to reintroduce the heavy quark kinetic energy and hyperfine interactions to the Hamiltonian. The wave function can be written in an expansion in powers of $1/m_Q$ as follows

$$\phi_M^{\text{NR}} = \phi_\infty^{\text{NR}} + \frac{1}{m_Q}(\phi_{\text{KE}}^{\text{NR}} + d_M \phi_{\text{HF}}^{\text{NR}}) + \mathcal{O}\left(\frac{1}{m_Q^2}\right). \quad (17)$$

The functions $\phi_{\text{KE}}^{\text{NR}}$ and $\phi_{\text{HF}}^{\text{NR}}$ arise from the effects of the kinetic energy and spin-spin hyperfine terms, respectively. They have been defined to be independent of m_Q . Note that $4(\mathbf{S}_c \cdot \mathbf{S}_d) = (-3, 1)$ for (M, M^*) is $-d_M$, which was defined in the previous section. Simply solving the Schrödinger equation including the $1/m_Q$ terms leads to contributions of the subleading-mass terms to all orders in $1/m_Q$. The functions $\phi_{\text{KE}}^{\text{NR}}$ and $\phi_{\text{HF}}^{\text{NR}}$ can be isolated using perturbation theory, where

$$\phi_{\text{KE}}^{\text{NR}}(\mathbf{r}) = \sum_{n \neq \infty} \frac{\phi_n^{\text{NR}}(\mathbf{r})}{E_n - E_\infty} \int d^3 \mathbf{r}' \phi_n^*(\mathbf{r}') \frac{\nabla^2}{2} \phi_\infty^{\text{NR}}(\mathbf{r}') \quad (18)$$

and

$$\phi_{\text{HF}}^{\text{NR}}(\mathbf{r}) = \frac{1}{4} \sum_{n \neq \infty} \frac{\phi_n^{\text{NR}}(\mathbf{r})}{E_n - E_\infty} \int d^3 \mathbf{r}' \phi_n^*(\mathbf{r}') \frac{8\pi\alpha_s}{3m_q} \delta^3(\mathbf{r}) \phi_\infty^{\text{NR}}(\mathbf{r}'). \quad (19)$$

In Eqs. (18) and (19) the set of functions $\phi_\infty, \phi_1, \phi_2, \dots$ represents the complete set of solutions to Eq. (15) with the unperturbed Hamiltonian in Eq. (14). In practice it proves easier to numerically find the piece of the solution to the full Hamiltonian linear in $1/m_Q$ than to directly apply Eqs. (18) and (19).

The constants G_1 and G_2 defined in Eq. (8) are related to the wave function corrections by

$$G_1 = \frac{\phi_{\text{KE}}^{\text{NR}}(0)}{\phi_\infty^{\text{NR}}(0)} \quad (20)$$

and

$$G_2 = \frac{\phi_{\text{HF}}^{\text{NR}}(0)}{2\phi_\infty^{\text{NR}}(0)}. \quad (21)$$

The quark model calculation to order $1/m_Q$ reproduces the form of the heavy quark result in Eq. (8) with the exception of the term proportional to $\tilde{\Lambda}$, which is absent in the model calculation. This missing term manifests one of the limitations of the constituent quark model. It can be understood as follows: the factor $\tilde{\Lambda} = \bar{\Lambda} - m_q$ arises in a process with $q^2 = m_M^2$, which is large compared to Λ_{QCD} . The relevant light quark mass m_q should therefore be the current quark mass, which means

$$\tilde{\Lambda} = \bar{\Lambda} - m_q^{\text{current}} \simeq \bar{\Lambda}. \quad (22)$$

The quark model only knows about constituent quarks, however, which would give

$$\tilde{\Lambda}^{\text{quark model}} = \bar{\Lambda} - m_q^{\text{constituent}} = 0. \quad (23)$$

This facet of the quark model calculation is wrong. Fortunately, the deficiency can be compensated for by manually including the $\tilde{\Lambda}$ term.

A more serious problem arises in the calculation of the hyperfine correction to the wave function ($\phi_{\text{HF}}^{\text{NR}}$). A straightforward evaluation of the sum in Eq. (19) shows that $\phi_{\text{HF}}^{\text{NR}}$ (and consequently G_2) diverges. The delta-function potential is too singular for the Schrödinger equation so the wave function at the origin diverges, even at leading order in perturbation theory. Although it is possible to regulate this singularity through a variety of methods, the resulting calculation depends critically on the method chosen. Since the effect of the perturbation on the wave function (eigenfunction) is infinite, one might naively expect that the effect of the perturbation on the mass (eigenvalue) would also be infinite. Then the correction to the heavy particle mass, which is measurable through the B - B^* mass splitting, could be calculated in the regularized theory and subsequently be used to fix the regularization parameter by fitting to the measured mass splitting. Unfortunately, this procedure fails because the effect of the hyperfine perturbation gives a finite eigenvalue correction, even though it gives an infinite eigenfunction correction.

I will assume that the hyperfine contribution, and subsequently G_2 , is negligible compared to the kinetic energy contribution with the following justifications: Qualitatively, one can compare the terms in the Eq. (19) sum with the terms in the Eq. (18) sum. In both cases the first terms in the series, *i.e.*, the contributions of the lowest-lying excited states, are larger in magnitude than any other terms. Comparing only these first few terms, the kinetic energy perturbation is much larger than the hyperfine perturbation. However, the large- n terms in the hyperfine sum fall only like $1/n$, so the sum diverges, whereas the terms in the kinetic sum fall quickly enough for the sum to converge. From this it seems plausible that an appropriately regularized calculation will yield $|G_2| < |G_1|$. Furthermore, two QCD sum rule calculations [21, 12] give $|G_2| \ll |G_1|$. Therefore, it is reasonable to assume that the hyperfine interaction can be neglected in this calculation.

Fortunately, the dominant G_1 term is easily calculable in the nonrelativistic model. The effect of (re-)introducing the heavy quark kinetic energy can be incorporated in the usual way by substituting the reduced mass m_{red} ,

$$\frac{1}{m_{\text{red}}} = \frac{1}{m_q} + \frac{1}{m_Q}, \quad (24)$$

for the light quark mass m_q . However, simply making the substitution introduces corrections to all orders in $1/m_Q$. This is a problem because the heavy quark kinetic energy $p^2/(2m_Q)$ is only correct to leading order in $1/m_Q$.[†] Taylor-expanding $\phi(0)$ as a function of m_{red}

$$\phi(r) = \phi_{\infty}(r) + (m_{\text{red}} - m_q) \frac{\partial \phi_{\infty}(r)}{\partial m_q} + \mathcal{O}[(m_{\text{red}} - m_q)^2], \quad (25)$$

[†]Which, of course, leads one to wonder about higher-order corrections to the light quark kinetic energy, which do not converge, since typical values of p are of the same order as the constituent light quark mass m_q . Concerns such as these inevitably lead to a model with relativistic light-quark kinematics such as the one in the following section.

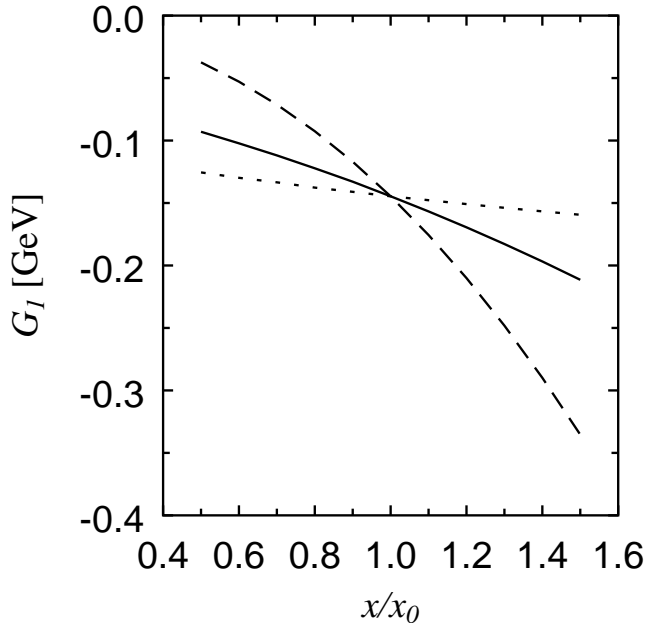


Figure 3: Parameter dependence of G_1 calculated using the nonrelativistic model. The parameters (x) are α_s (solid line), m_q (dashed line) and a (dotted line).

yields the following expression for G_1

$$G_1 = \frac{m_q^2}{\phi_\infty(0)} \frac{\partial \phi_\infty(r)}{\partial m_q}. \quad (26)$$

Numerically, it is easier to treat the heavy quark kinetic energy as a perturbation, as described above.

The numerical calculation gives $G_1 = -0.14$ GeV. Fig. 3 displays the parameter dependence of the calculation, showing that varying the parameters does not allow for values of G_1 much larger (in absolute value) than 0.3 GeV.

4 Semirelativistic Model Calculation

The idea of the semirelativistic model is to remove the most obviously incorrect part of the nonrelativistic quark model, the nonrelativistic form of the kinetic energy for the light quark. Take the nonrelativistic quark model Hamiltonian in the heavy-quark limit, Eq. (14), and make the substitution

$$\frac{p^2}{2m_q} \rightarrow \sqrt{p^2 + m_q^2}. \quad (27)$$

The resulting wave equation,

$$\sqrt{p^2 + m_q^2} \psi = (E - V) \psi, \quad (28)$$

is known as the spinless Salpeter equation [29]. It follows from the full Bethe-Salpeter equation in the spin-independent and instantaneous-interaction approximation. The spin-independence is justified by the heavy-quark limit. The instantaneous-interaction approximation is a limitation of the model. Duncan, Eichten and Thacker have shown [30] that the spinless Salpeter equation produces wave functions which are very similar to those obtained from lattice calculations.

If the substitution of the relativistic kinetic energy is the only change made to the model of the previous section, the potential in Eq. (28) is

$$V = -\frac{4\alpha_s}{3r} + ar. \quad (29)$$

Unfortunately, the resulting solution to Eq. (28) diverges at the spatial origin, which results in an infinite value for F when calculated with Eq. (16). One might be tempted to ascribe this divergence to the phenomenological part of the potential. However, the divergence depends only on the coulombic part of the potential; it is independent of the phenomenological linear term. Wave function divergence at the spatial origin is actually a general problem affecting relativistic wave equations. For example, the solution to the Dirac equation for the Coulomb potential behaves like

$$\Psi \sim (2m\alpha r)^{\sqrt{1-\alpha^2}-1} \quad (30)$$

for small r . While the divergence in Eq. (30) is very weak, the divergence of the solution to the spinless Salpeter equation with the potential in Eq. (29) is much stronger,

$$\Psi \sim r^{-\frac{4\alpha_s}{3\pi}}, \quad (31)$$

as can be seen with the methods of Ref. [31].

The singularity in the wave function is clearly related to the singularity of the $1/r$ potential. If we consider instead the one-loop single gluon exchange potential [32,33], the net effect is to replace the constant value of α_s in Eq. (31) with the one-loop running value of $\alpha_s(1/\Lambda r)$. Leaving the phenomenological linear term unchanged, the potential is now

$$V = -\frac{4\alpha_s(1/\Lambda r)}{3r} + ar, \quad (32)$$

where

$$\alpha_s(1/\Lambda r) = \frac{4\pi}{\beta_0 \ln(1/\Lambda^2 r^2)}, \quad (33)$$

which has a much milder singularity at the origin. The resulting wave function still diverges, but only logarithmically. Again following a derivation similar to that in Ref. [31], one can show that the small- r behavior of the solution to the spinless Salpeter equation with the potential in Eq. (32) is

$$\phi_\infty^{\text{SR}}(r \rightarrow 0) \sim [-\ln(\Lambda r)]^{4/3\beta_0}. \quad (34)$$

The physical decay constant is a product of a perturbative coefficient which depends on a scale μ with the low-energy parameter $F(\mu)$, as is shown in Eq. (6), which is correct to leading-log order. The logarithmic behavior of the wave function in Eq. (34) is of the right form to cancel the $\ln(\mu)$ dependence of the perturbative coefficient that would be obtained if we had only considered single gluon exchange (*i.e.*, the vertex correction) in the perturbative coefficient in Eq. (6). This is as it should be, since the solution to the wave equation can be considered an infinite series of single-gluon exchanges. The full one-loop perturbative calculation also includes the propagator corrections for the light and heavy quarks, but these effects are not present in this model. A better model would produce the full $\ln(\mu)$ dependence of $F(\mu)$.

In the present case, the correct quantity to compare with the nonrelativistic wave function at the origin is the semirelativistic wave function at the origin without the logarithmic divergence, which should cancel with the μ dependence of the perturbative correction in the full calculation. Then the quantity

$$F_0 = \lim_{r \rightarrow 0} \frac{\phi_\infty^{\text{SR}}(r)}{\ln(1/\Lambda r)^{4/3\beta_0}} \quad (35)$$

should be compared to F as calculated in the nonrelativistic model.

A subtlety arises in the one-loop potential because $\alpha_s(1/\Lambda r)$ diverges for $r \sim \Lambda^{-1}$. This unphysical behavior arises from the nonperturbative nature of QCD at long distances, and as such should be swept into the phenomenological part of the potential. I have followed the procedure used by Peskin and Strassler [34] to smoothly turn off the running of α_s at long distances. The prescription is to make the substitution $\Lambda r \rightarrow \kappa \tanh(\Lambda r/\kappa)$ in the running of α_s . The results are insensitive to the precise value of the parameter κ , which I set to 0.5 for the results I present here.

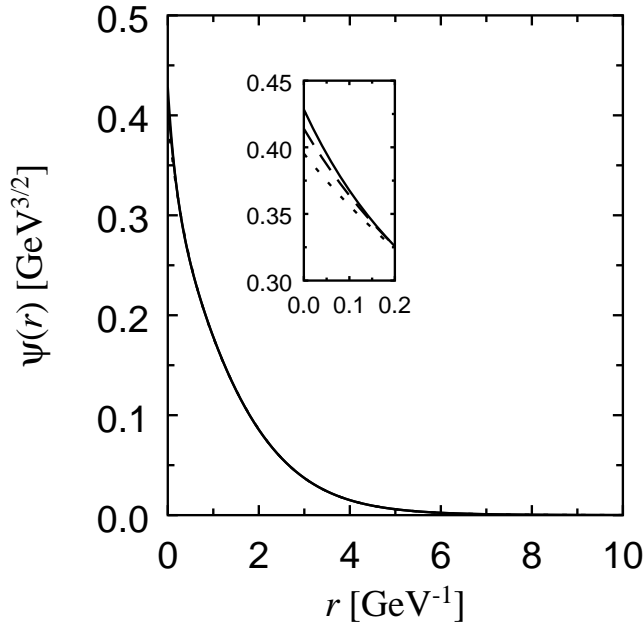


Figure 4: Semirelativistic wave function calculated using 10 (dotted line), 15 (dashed line) and 20 (solid line) pseudohydrogenic basis functions. The inset shows that the numerical calculation fails to converge at the origin, where the wave function diverges logarithmically.

Fig. 4 shows the numerical solution to the spinless Salpeter equation with the one-loop potential. The values of m_q and a are the same as in the previous section. There is a subtlety in choosing m_q in this model. In one picture the constituent quark mass arises from the relativistic “jiggle” of the light quark in the hadron. In another picture, the constituent quark mass arises from chiral symmetry breaking. Although these schemes are not necessarily mutually exclusive, the former requires using the current light quark mass in this model, while the latter requires using the constituent mass. Here I have chosen the latter option. It should be noted, however, that the results do not depend very strongly on the light quark mass, so choosing the former option would not qualitatively change the results. I have chosen $\Lambda = 237$ MeV so that the one-loop potential (Eq. (32)) is the same as the original potential (Eq. (29)) at $r = 1$ GeV $^{-1}$. Fig. 5 displays the sensitivity of resulting value of F_0 to the model parameters. The central value, $F_0 = 0.67$ GeV, is only about 20% higher than the value of F obtained in the nonrelativistic model.

Calculating the subleading terms $\tilde{\Lambda}$, G_1 and G_2 is quite similar to the nonrelativistic calculation. The $\tilde{\Lambda}$ term has to be included by hand, just as before. The hyperfine effect, G_2 , which was problematic in the nonrelativistic model, is also problematic in the semirelativistic model. Even though the one-loop potential, with its milder $r \rightarrow 0$ singularity, helped deal with the divergence at the origin of ϕ_∞^{SR} , it does not alleviate the additional singularities in the hyperfine potential. The one-loop hyperfine potential [32, 33],

$$V_{\text{HF}} = \frac{32\pi}{3}\alpha_s(\mu) \left\{ \left[1 + \frac{\alpha_s}{\pi} \left(\frac{5}{12}\beta_0 - \frac{11}{3} + \frac{15}{24} \ln \frac{m_Q}{m_q} \right) \right] \delta^3(\mathbf{r}) + \frac{\alpha_s}{\pi} \left(\frac{21}{8} - \frac{\beta_0}{4} \right) \left[\frac{1}{2\pi} \frac{1}{r^3} + 2\gamma_E \delta^3(\mathbf{r}) \right] \right\}, \quad (36)$$

contains terms just as singular as the tree-level hyperfine potential. This means that even after the original divergence at the origin is regulated, the hyperfine potential will introduce a new divergence. This result can be anticipated from the perturbative calculation in the effective theory, where $G_2(\mu)$ gets a perturbative coefficient in Eq. (11) beyond that of $F(\mu)$. As a rule, terms which have renormalization coefficients with non-trivial $\ln(\mu)$ -dependence diverge in the semirelativistic model. G_1 , which is protected from renormalization

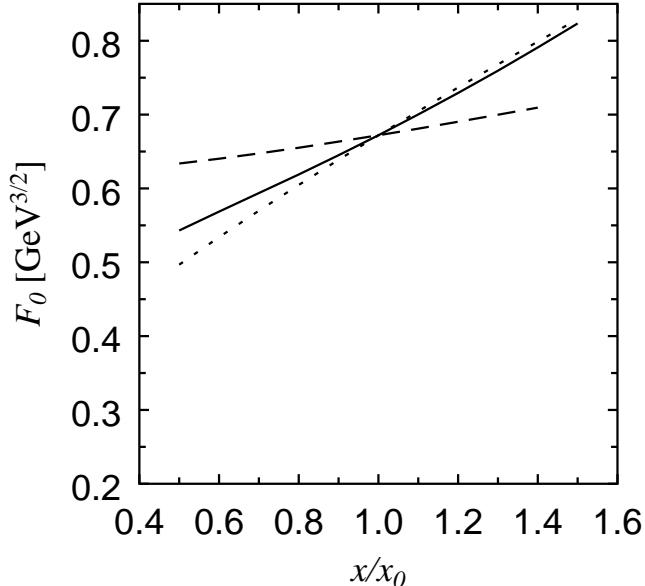


Figure 5: Parameter dependence of F_0 calculated using the semirelativistic model. The nominal values (x_0) are (solid line) $\Lambda = 0.237$, (dashed line) $m_q = 0.33$ GeV, and (dotted line) $a = 0.18$ GeV².

by reparameterization invariance, does not diverge in the model calculation.

Although the semirelativistic model G_2 calculation seems to be more tractable than the similar problem in the nonrelativistic model, the calculation is extremely sensitive to the small- r dependence of the wave function. This is precisely where the numerical method breaks down, so the calculation is not technically feasible. Neither the nonrelativistic nor semirelativistic models in present form give definite predictions for G_2 . Fortunately, as argued in the previous section, indications are that G_2 is negligibly small compared to G_1 .

The kinetic energy term, G_1 , can easily be calculated by treating the $p^2/2m_Q$ term as a perturbation. (The interpretation as a reduced mass effect mentioned for the nonrelativistic model does not translate to the semirelativistic model, so Eq. (26) no longer holds.) The result is displayed in Fig. 6, once again showing dependence on the various parameters.

Here the two models give dramatically different results. G_1 is several times larger in the semirelativistic model than it is in the nonrelativistic model. Also the parameters are correlated such that the two models cannot be made qualitatively similar by changing any combination of the parameters.

5 Discussion

It is convenient to define a quantity g_M , such that

$$f_M = F \left(1 + \frac{g_M}{m_Q} \right) + \mathcal{O} \left(\frac{1}{m_Q^2} \right). \quad (37)$$

In Table 1 I have summarized the results of the two model calculations, including g_M for pseudoscalar mesons, g_P . (In general, the pseudoscalar meson's g_P will be different from the vector meson's g_V due to the effects of the hyperfine operator, G_2 . Since the model calculations neglect the hyperfine contribution, $g_M = g_P = g_V$ for these calculations.) I have used $\bar{\Lambda} = m_q = 0.33$ GeV to calculate g_P . Note that g_P in the nonrelativistic calculation is equal to the naive guess from the introduction. This is actually fortuitous, because the contribution of the $\tilde{\Lambda}$ term, which accounts for half of the value, is not included in the naive

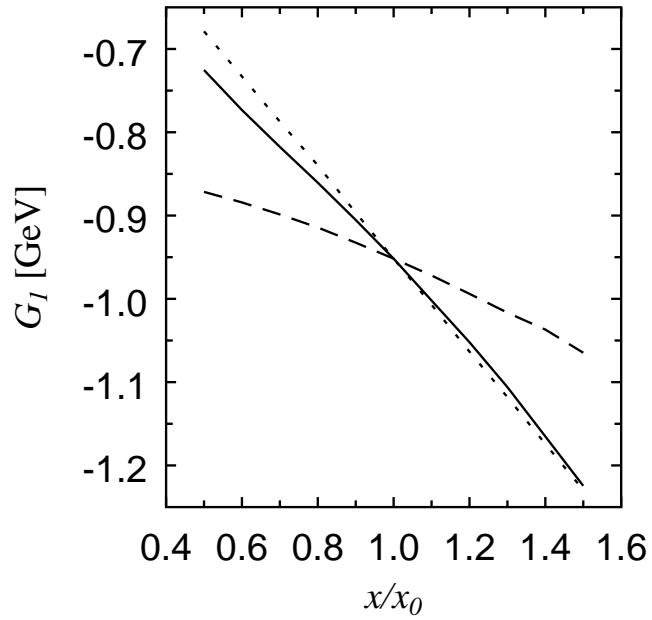


Figure 6: Parameter dependence of G_1 calculated using the nonrelativistic model. The parameters (x) are Λ (solid line), m_q (dashed line) and a (dotted line).

Table 1: Comparison of the nonrelativistic and semirelativistic models.

	$F (F_0) [\text{GeV}^{3/2}]$	$G_1 [\text{GeV}]$	$g_P [\text{GeV}]$
nonrelativistic	0.55	-0.14	-0.31
semirelativistic	0.67	-0.95	-1.12

model. As stated in the introduction, lattice calculations indicate that $g_P \approx 1$ GeV. The semirelativistic calculation is consistent with that result, but the nonrelativistic calculation is not. The difference is due to the G_1 contribution.

The nonrelativistic and semirelativistic values of G_1 differ not just quantitatively, but qualitatively. This qualitative difference would be completely obscured by a model comparison done in the traditional way, *i.e.*, by calculating only the decay constant and including the heavy quark mass effects to all orders. The heavy quark mass suppresses the effects of the G_1 term in the decay constant itself. The (heavy quark suppressed) large difference at subleading order also tends to compensate the smaller difference between the two models at leading order.

The origins of the discrepancy between the two models can be understood as follows: For small p , the two Hamiltonians are the same. For large p , however, the kinetic energy term grows like p^2 nonrelativistically, but only like p relativistically. This means that the semirelativistic Hamiltonian is less confined in momentum space than the nonrelativistic Hamiltonian, *i.e.*, the semirelativistic wave function is more spread out in momentum space than the nonrelativistic wave function. Because the wave functions are normalized, an increase of the wave function at large momentum must be compensated by a decrease at small momentum, so the difference between the wave functions tends to cancel for $\psi(\mathbf{r} = 0)$, which can be written in p -space as

$$\psi(\mathbf{r} = 0) = \int d^3\mathbf{p} \psi(\mathbf{p}). \quad (38)$$

G_1 , however, is proportional to $\phi_{\text{KE}}(\mathbf{r} = 0)$, which can be written as

$$\phi_{\text{KE}}^{\text{NR}}(\mathbf{r}) = \sum_{n \neq \infty} \frac{\phi_n^{\text{NR}}(\mathbf{r})}{E_n - E_\infty} \int d^3\mathbf{p}' \phi_n^*(\mathbf{p}') \frac{p'^2}{2} \phi_\infty^{\text{NR}}(\mathbf{p}'). \quad (39)$$

The p^2 factor in the integral emphasizes the large- p differences in the wave functions, making G_1 a sensitive probe of the large-momentum tail of heavy-light wave functions. This, in turn, leads to the following rule: Quantities which are sensitive to the large-momentum shape of wave functions are dramatically underestimated by the nonrelativistic quark model.

This rule has implications for other processes. In particular, it indicates that nonrelativistic quark model calculations of processes at large momentum transfer seriously underestimate the overlap of meson wave functions. An important example that has received much interest lately is the process $B \rightarrow K^* \gamma$. In the B meson's rest frame the K^* has ≈ 1.3 GeV of momentum, which is large compared to the typical widths of meson wave functions in the nonrelativistic quark model. This means that the overlap is dominated by the tails of the wave functions, which I have just shown to be poorly described by the nonrelativistic quark model.

This work not only provides an explanation for the conflict between the nonrelativistic quark model and other estimates for the heavy-quark symmetry breaking behavior in decay constants, it also suggests a qualitative solution to an earlier conflict: In Ref. [28], I calculated heavy-quark symmetry-violating corrections to form factors in $B \rightarrow D^{(*)} l \nu$ transitions. The predictions for the effects of the heavy-quark kinetic energy operator in were an order of magnitude smaller than a QCD sum rule calculation [35] of the same effect. This work shows that the nonrelativistic quark model dramatically underestimates the effect of the kinetic energy operator, in this case by a factor of 6. In the meantime, Neubert [36] has derived a theorem showing the sum rule used in Ref. [35] overestimate the effects of the same operator. While an explicit calculation is needed for both, it appears that the two different types of models should now be in qualitative agreement.

6 Conclusions

The nonrelativistic quark model provides a very simple picture of hadronic physics. While the picture is clearly too simple, it does yield insight into the structure of hadrons. Calculating decay constants in

the nonrelativistic quark model and a simple semirelativistic generalization shows how the nonrelativistic quark model can work reasonably well overall, yet fail to describe important details. This calculation shows that the nonrelativistic quark model does conflict with lattice and QCD sum rule predictions for the size of heavy quark symmetry-breaking effects in heavy-light decay constants. However, this conflict can be removed by going to a similar model with relativistic light quark dynamics. Comparing the two models shows that the nonrelativistic quark model should be expected to fail for calculations which are sensitive to the large-momentum tails of wave functions.

Acknowledgments

I would like to thank M.G. Olsson for helpful discussions. This research was supported in part by the University of Wisconsin Research Committee with funds granted by the Wisconsin Alumni Research Foundation, and in part by the U.S. Department of Energy under grant DE-FG02-95ER40896.

References

- [1] W. Lucha, H. Rupprecht, and F. F. Schoberl, Phys. Rev. D **46**, 1088 (1992).
- [2] Y. I. Azimov, L. L. Frankfurt, and V. A. Khoze, Pis'ma v Zh. Eksp. Teor. Fiz. **24**, 373 (1976), [JETP Lett. **24**, 338 (1976)].
- [3] M. B. Voloshin and M. A. Shifman, Yad. Phys. **45**, 463 (1987), [Sov. J. Nucl. Phys. **45**, 292 (1987)].
- [4] H. D. Politzer and M. B. Wise, Phys. Lett. B **206**, 681 (1988), ; **208**, 504 (1988).
- [5] S. Aoki *et al.*, Prog. Theor. Phys. **89**, 131 (1993).
- [6] D. Acosta *et al.*, Phys. Rev. D **49**, 5690 (1994).
- [7] J. Bai *et al.*, Technical Report No. SLAC-PUB-95-6746, SLAC (unpublished).
- [8] S. Hashimoto, Phys. Rev. D **50**, 4639 (1994).
- [9] A. Abada, Preprint LPTHE-ORSAY-94-79, Orsay, (unpublished), hep-ph 9409338.
- [10] C. Bernard *et al.*, Preprint FSU-SCRI-95C-28, Florida State University, (unpublished), hep-ph 9503336.
- [11] R. M. Baxter *et al.*, Preprint EDINBURGH-93-526, Edinburgh, (unpublished), hep-lat 9308020.
- [12] P. Ball, Nucl. Phys. B **421**, 593 (1994).
- [13] N. Isgur, D. Scora, B. Grinstein, and M. B. Wise, Phys. Rev. D **39**, 799 (1989).
- [14] H. Georgi, Phys. Lett. B **240**, 447 (1990).
- [15] E. Eichten and B. Hill, Phys. Lett. B **234**, 511 (1990).
- [16] M. Neubert, Phys. Rept. **245**, 259 (1994).
- [17] A. F. Falk and B. Grinstein, Phys. Lett. B **247**, 406 (1990).
- [18] A. F. Falk, B. Grinstein, and M. E. Luke, Nucl. Phys. B **357**, 185 (1991).
- [19] E. Eichten and B. Hill, Phys. Lett. B **243**, 427 (1990).
- [20] M. Luke and A. V. Manohar, Phys. Lett. B **286**, 348 (1992).
- [21] M. Neubert, Phys. Rev. D **46**, 1076 (1992).
- [22] V. Matveev, B. Struminskii, and A. Tavkhelidze, Report P-2524, Dubna (unpublished).
- [23] H. Pietschmann and W. Thirring, Phys. Lett. **21**, 713 (1966).
- [24] R. V. Royen and V. Weisskopf, Nuovo Cimento A **50**, 617 (1967).
- [25] R. V. Royen and V. Weisskopf, Nuovo Cimento A **51**, 583(E) (1967).
- [26] H. Krasemann, Phys. Lett. B **96**, 397 (1980).
- [27] D. Scora and N. Isgur, Preprint CEBAF-TH-94-14, CEBAF, (unpublished), hep-ph 9503486.

- [28] J. F. Amundson, Phys. Rev. D **49**, 373 (1994).
- [29] E. E. Salpeter, Phys. Rev. **87**, 328 (1972).
- [30] A. Duncan, E. Eichten, and H. Thacker, Phys. Lett. B **303**, 109 (1993).
- [31] L. Durand, Phys. Rev. D **32**, 1257 (1985).
- [32] S. Gupta, S. Radford, and W. Repko, Phys. Rev. D **34**, 201 (1986).
- [33] J. Pantaleone, S. Tye, and Y. J. Ng, Phys. Rev. D **33**, 777 (1986).
- [34] M. J. Strassler and M. E. Peskin, Phys. Rev. D **43**, 1500 (1991).
- [35] M. Neubert, Phys. Rev. D **46**, 3914 (1993).
- [36] M. Neubert, Phys. Lett. B **322**, 419 (1994).
- [37] I. Stakgold, *Green's Functions and Boundary Value Problems* (Wiley, New York, 1984).
- [38] E. J. Weniger, J. Math. Phys. **26**, 276 (1985).
- [39] S. Jacobs, M. G. Olsson, and C. S. III, Phys. Rev. D **33**, 3338 (1986).

Appendix

This appendix describes the method I used to obtain the numerical results in the text. While the Schrödinger equation can easily be solved with a wide variety of numerical techniques, the spinless Salpeter equation is much more difficult. The position-space representation of the spinless Salpeter equation contains the problematic $\sqrt{-\nabla^2 + m_q^2}$ operator, while the momentum-space representation contains a complicated convolution integral from the potential.

These problems can be avoided by using the Rayleigh-Ritz-Galerkin (RRG) method [37], which easily handles both the Schrödinger and the spinless Salpeter equations. RRG is an extension of the elementary variational method. In the variational method, one chooses a state parameterized by λ , then minimizes

$$E_{\text{var}} = \langle \lambda | \mathcal{H} | \lambda \rangle \quad (40)$$

with respect to λ . For reasonable choices of $|\lambda\rangle$, $E_{\text{var}}^{\text{min}}$ and $|\lambda^{\text{min}}\rangle$ form good approximations to the eigenvalue and eigenket, respectively. In the RRG method, one chooses an orthogonal set of n vectors, $|\lambda, i\rangle$ $i = 1 \dots n$, then minimizes

$$E_{\text{RRG}} = \langle \Psi | \mathcal{H} | \Psi \rangle, \quad (41)$$

where $|\Psi\rangle = c_i |\lambda, i\rangle$. One can calculate wave functions and energy eigenvalues arbitrarily well by choosing sufficiently large n . The problem is reduced to the numerically straightforward problems of calculating integrals and solving a matrix equation for the c_i 's.

The difficulties with the spinless Salpeter equation can be avoided in the RRG method by breaking up the expectation value of the Hamiltonian into kinetic and potential pieces,

$$\mathcal{H} = T + V, \quad (42)$$

then writing Eq. (41) as follows

$$E_{\text{RRG}} = \langle \Psi | p \rangle \langle p | T | p \rangle \langle p | \Psi \rangle + \langle \Psi | x \rangle \langle x | V | x \rangle \langle x | \Psi \rangle. \quad (43)$$

The resulting integrals are straightforward as long as the representations of the $|\lambda, i\rangle$'s are known in both position and momentum space.

For the calculations in this work I used two different bases: the harmonic oscillator basis and the confined pseudohydrogenic basis. The former are standard; the latter were developed in Ref. [38] and first used for the spinless Salpeter equation in Ref. [39]. All convergent results are independent of basis. The two different bases act as a cross-check. Since the spinless Salpeter wave function diverges at the origin, the two methods do not agree in a small region around the origin. The inset in Fig. 4 shows the failure to converge in the pseudohydrogenic basis. The same plot with the harmonic oscillator basis is different in the vicinity of the origin. Nevertheless, the limiting procedure in Eq. (35) provides a finite quantity which is basis-independent. All the results in the text are independent of basis.